

Riding the Airways: Ultra-Wideband Ambient Backscatter via Commercial Broadcast Systems

Chouchang Yang, Jeremy Gummesson, and Alanson Sample

Disney Research Pittsburgh, PA 15213

email: {jack.yang, alanson.sample}@disneyresearch.com

Abstract—Communication costs dominate the energy consumption, and ultimately limit the utility, of low power devices and sensor nodes. Backscatter communication based on deliberate and ambient sources has the potential to radically alter this paradigm by offering two to three orders of magnitude better communication efficiency (in terms of nJ/Bit) than conventional radio architectures. Initial work on ambient backscatter shows promising results but has focused on narrow band operation in well controlled laboratory settings.

The goal of this work is to enable the ubiquitous deployment of ultra-low power nodes that communicate via ambient backscatter to wired Universal Backscatter Readers, in real-world environments. This is accomplished through ultra-wideband backscatter techniques that leverage the breath of commercial broadcast signals in the 80 MHz to 900 MHz range from FM radios, digital TVs, and cellular networks. Additionally the use of powered Universal Backscatter Readers allows a network of ultra-low power nodes to operate on ambient carriers as low as -80 dBm, which is typical for indoor home and office environments. For the first time we demonstrate the simultaneous use of 17 ambient signal sources to achieve node-to-reader communication distances of 50 meters, with data rates up to 1 kbps.

Index Terms—Ultra-Wideband, Ambient Backscatter Communication, Sensor Node, Energy Harvesting

I. INTRODUCTION

Battery powered wireless sensors serve as the “end-effector” of the Internet of Things. Their small size and low cost allows them to be attached to a wide variety of objects and stream data back to a gateway for connection to the Cloud [1], [2]. However, as we move towards connecting the next billion wireless devices to the internet, the cost of batteries and the burden of replacing them becomes prohibitively expensive and unmanageable at scale. While energy harvesting has shown promising results for outdoor environments with a high degree of harvestable power [3], the power consumption of traditional sensor nodes is not well suited for the relatively small amounts of available power in our indoor environments [4].

Therefore, in order to enable the ubiquitous and long-term deployment of wireless sensing and computing devices, we must rethink wireless sensor platform architecture in order to radically reduce power consumption. A compelling alternative to traditional, power hungry active radios (consisting of oscillators, mixers, power amplifiers, etc.) is RF backscatter communication, which offers 2 to 3 orders of magnitude in power savings in terms of Joules/bit [5].

Backscatter communication has been successfully used in UHF systems where RFID readers transmit data and RF power

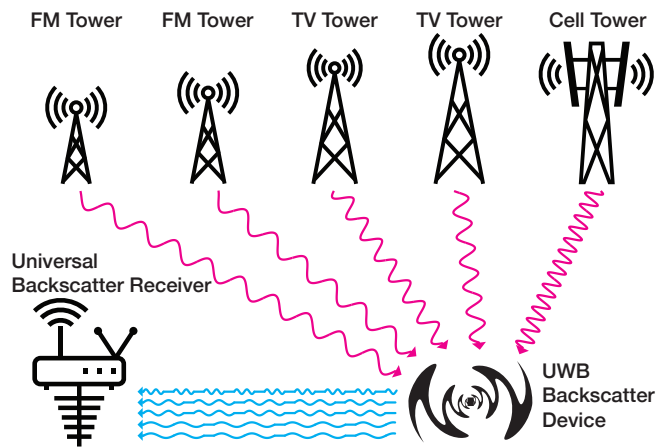


Fig. 1. Ultra-wideband ambient backscatter systems consisting of multiple FM radio stations, Digital TV stations and cellular communication networks. Energy harvesting nodes with UWB antennas, reflects (i.e. backscatters) all ambient radio signals to the universal backscatter reader which combines these signal sources in order to increase robustness and boost read range.

to battery-free RFID tags. Instead of actively generating RF signals to respond back to the reader, the tag modulates its antenna's load impedance thereby reflecting the RFID reader's carrier wave back to the reader to send data. This ultra low power architecture has enable battery-free sensing and computing tags compatible with off-the-shelf UHF RFID readers [6], [7]. However, UHF RFID sensor networks have seen limited deployment due to the short read range of RFID tags (5-10 m), and the need to densely deploy readers, which increases cost and causes reader-to-reader interference [5], [8].

An alternative approach is to use ambient radio waves—which are already present in our indoor environments—as a medium to backscatter data to a wired backscatter receiver (i.e. internet gateway). This approach allows wireless sensor nodes to retain the low power nature of backscatter radios while reusing existing radio spectrum and thus eliminating the need for dedicated RF transmitters. Demonstrations have shown that it is possible to achieve battery-free node-to-node communication using a single TV station [9], [10] and node-to-gateway communication using WiFi signals [11], [12]. However, backscatter transmission distance is typically limited to 1-5 meters or requires an artificial, high power RF source to boost read range [13], [14].

Instead of focusing on one particular signal source or communication protocol, this work takes an alternative approach

that uses all available ambient radio sources from FM radio stations, to digital TV stations, all the way up to cellular networks for backscatter communication. This technique is depicted in Figure 1, which shows several commercial broadcast systems operating at frequencies from 80 MHz to 900 MHz. Here the energy harvesting nodes use an UWB antenna and broadband switch to backscatter all ambient sources to a Universal Backscatter Reader (UBR). The reader then selects the strongest set of RF sources in the environment and combines them when decoding the backscatter data.

This approach has a number of key advantages compared to narrow band systems. Primarily, combining multiple backscatter channels both mitigates dead zones caused when using incoherent backscatter receivers and boost the signal-to-noise ratio, thus substantially improving the sensitivity of a backscatter reader. This enables our system to operate on real-world ambient radio sources as low as -80 dBm, which is the minimum required ATSC digital TV receiver sensitivity [15]. This increased sensitivity to ambient signal power means that UWB ambient backscatter systems can be deployed in most locations or geographic regions without the need to re-tune hardware for a particular frequency. For example, if the signal is strong enough to be received by a digital television then it should also be strong enough to be used by an ambient backscatter node. Finally, the increased signal-to-noise ratio offered by UWB operation also results in significantly longer read ranges using ambient signal sources than narrow band systems without the aid of active RF boosters.

This paper focuses on the building blocks and system architecture needed to enable ultra wide-band backscatter communication. We begin with a system overview and then describes the signal processing pipeline used to decode the backscatter signals. This is followed by a maximum ratio combining technique that includes carrier interference cancellation, which is validated against benchmark tests. Finally a real-world test of our UWB ambient backscatter system is conducted in an office environment and shows read ranges of 22 meters when operating from ambient signals generated by local towers and read ranges of 50 meters when operating from ambient signals generated by mobile phone up-link traffic.

II. RELATED WORK & CONTRIBUTIONS

While the underlying physics and propagation models of backscatter are well known in the UHF RFID community [16], [17], researchers are now focusing on new system level designs and are pushing the application space beyond inventory asset tracking. Since there are a wide variety of conventional and ambient backscatter approaches that are being investigated in literature it is useful to articulate our underlying assumptions and draw a distinction between previous work. As stated earlier, this work focuses on ultra-wideband backscatter communication –using commercial broadcast radio signals– where energy harvesting nodes send data to powered Universal Backscatter Receivers that serve as gateways to the Internet.

A significant amount of previous work on ambient backscatter has focused on 2.4 GHz Wi-Fi since it has the advantage

of being a single band system that is deployed ubiquitously in homes and offices worldwide. However, from the perspective of the physical layer the discontinuous nature of Wi-Fi traffic means that data from a wireless node can only be backscattered when there is sufficient Wi-Fi traffic. To overcome this issue large amounts of artificial traffic must be generated in order to have enough RF carrier for backscatter communication [11]. An alternative approach is to use an active 2.4 GHz transmitter to generate a continuous single tone, thus creating an RF medium for backscatter [13]. This is similar to traditional UHF RFID readers, except that the RF transmitter and receiver are physically separated as opposed to being combined into a single unit. This approach has a secondary benefit since it is easier to decode backscatter data on a constant envelope waveform compared to a time varying one.

Ambient backscatter systems based on TV signals have been used for near-field node-to-node communication [9]. One way to boost communication range is to use multiple antennas with active interference cancellation [10]. Here Parks et. al. developed a MIMO node that demonstrated an impressive backscatter read range using a single TV channel; the signal was captured by a USRP and replayed at power levels of -25 dBm to 0 dBm. However, these power levels are not typical of indoor TV signal levels, which are usually in the -80 to -50 dBm range [15].

The focus of this work is to develop an ultra-wideband backscatter communication system capable of transmitting data over long distances (10s of meters) while operating from ambient radio sources with power levels typically found in indoor environments (-80 to -39 dBm). To accomplish this we have developed an energy harvesting sensor node that backscatters all signal sources from 80 to 900 MHz for communication. We also developed a Universal Backscatter Receiver using Software-Defined Radios to decode the backscatter data the rides on top of analog FM radio, digital TV and cellular communication protocols. Finally, we developed a maximum ratio combining algorithm with carrier interference compensation that combines all backscatter channels to improve signal quality. Furthermore, since our system is wideband and operates at very low ambient power levels it can be deployed in a wide number of locations and regions without needing to be tied to a particular ambient transmission source. The contributions we make towards enabling ultra-wideband, ambient backscatter systems are as follows:

Contributions:

- UWB backscatter nodes that uses all ambient radio sources form 80MHz to 900MHz for communication.
- Backscatter decoding methods for FM Radio, ATSC Digital TV, CMDA2000 (up and down links) as well as UMTS (up and down links)
- Implementation of a maximum ratio combining technique with carrier interference cancellation
- Demonstration of the system operating in a multi-path rich office environment using 17 real world signal sources at power levels ranging from -80 to -39 dBm

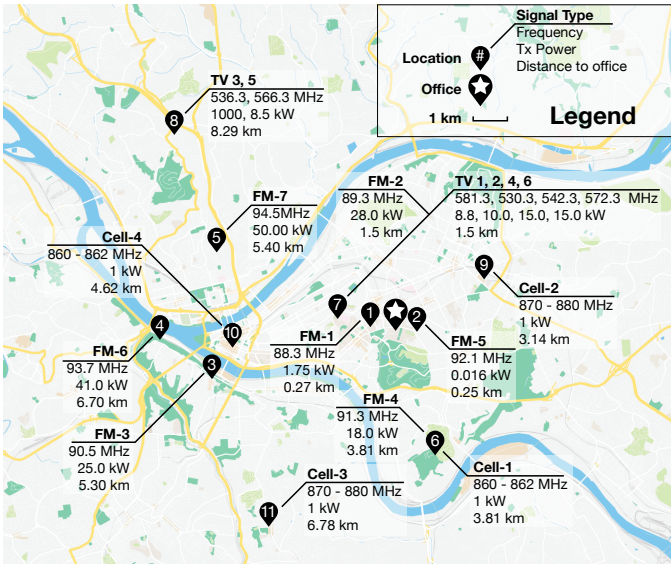


Fig. 2. Map of the FM, TV, and cellular towers used in this work annotated with: carrier frequency, transmit power, and distance to our lab denoted with an star. Our indoor office test environment does not have line-of-sight to any of the towers and ambient signal levels range from -32dBm to -90dBm. Including the two cell phones used to test CDMA2000 and UMTS, a total of 17 ambient radio sources are used in this work.

III. UWB AMBIENT BACKSCATTER SYSTEM OVERVIEW

As shown in Figure 1 our ultra-wideband backscatter system consist of three major pieces: 1) Ambient radio sources consisting of FM radio, Digital TV, and CDMA-based cellular networks which create the RF medium for backscatter communication. 2) Energy harvesting nodes capable of backscattering RF signals from 80 MHz to 900 MHz. 3) A Universal Backscatter Reader that is capable of decoding the backscatter communication that rides on top of RF signals transmitted by the three commercial broadcast systems. The following sections describe each of these components.

A. Ambient Radio Sources

There are a wide variety of radio sources that are omnipresent in our daily lives. While the ultra-wideband sensor nodes reflect all signals from 80MHz to 2.5GHz, this work specifically targets analog FM radio stations, ATSC digital TV stations and cellular networks consisting of CDMA2000 (up and down links) and UMTS (up and down links). While the use of other transmission frequencies and broadcast protocols are possible these radio systems are attractive since they cover a large portion of the RF spectrum allowing for sufficient diversity, are transmitted at high power levels ranging from a hundred watts to one megawatt, are widely deployed throughout the world and information on protocol encoding and tower locations is readily available.

Figure 2 shows the location of 15 ambient radio sources used in this work, which are transmitted from 11 radio towers around the greater Pittsburgh metro region. It should be noted that while some of the towers are quite close to our research facility (denoted with a star marker), their transmission power

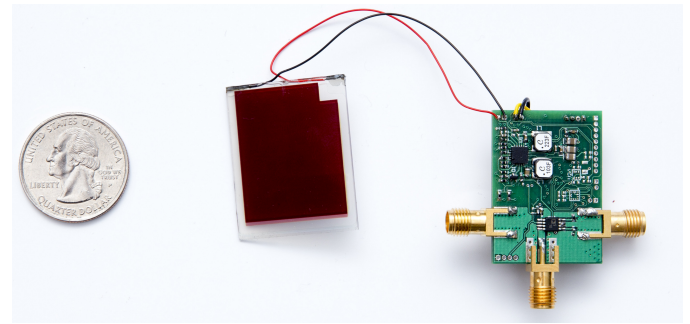


Fig. 3. Image of the ultra-wideband ambient backscatter node with solar cell for energy autonomous sensing and computing.

is actually quite low and does not artificially inflate the results. Our office does not have line of sight to any of the towers and thus the received signals are multipath in nature and are low in signal strength (-95 dBm to -39 dBm). In order to investigate CDMA2000 and UMTS up-links (i.e. phone to cell tower) ambient backscatter performance, two cell phones are employed as described in section VI, bringing the total count of ambient sources used in this study to 17.

B. UWB backscatter node

Figure 3 shows an image of an energy autonomous ultra-wideband backscatter sensor node. The node consists of an MSP430 ultra-low power microcontroller with onboard sensors including temperature, 3D acceleration, 3D compass, light level, and barometric pressure. The MSP430 modulates an Analog Devices ADG919 wideband switch to change the antennas load impedance from 50 ohms (absorbing all signals) to an electrical short (reflecting all signals) and thus is capable of backscattering signals from 15 KHz to 2.5 GHz. The nodes use a commercially available wideband antenna with sufficient performance from 470MHz to 900MHz and an electrically short monopole for FM backscatter. Although not the focus of this work, the nodes antenna can be unified into one element and optimized for size.

Finally since the power levels of the ambient radio waves available in our office are between -39 dBm and -95 dBm, it is not feasible to harvest enough RF energy for operation. Instead an 8.9 cm² die select sensitive solar cell – that has been optimized for low light conditions – is used as a power source, along with a Texas Instruments BQ25570 PMIC for energy harvesting and power conversion, and a 1 mF super capacitor for energy storage. Initial results show that energy neutral operation can be achieved at low indoor light levels of 570 Lux, while transmitting barometer and temperature readings every 26 seconds. This heavily duty cycled workload has an average power consumption of 1.3 μ W. In order to minimize “on time” during backscatter communication the MCU was put to sleep between symbol transitions. This resulted in a radio transmission efficiency of 1.9 nJ per bit when transmitting a PN sequence of length 63 at a rate of 10kHz. This equates to a 30.2 pJ per chip transition, which is similar to other backscatter systems that do not use PN sequences [14].

C. Universal Backscatter Reader

The UWB backscatter node is a minimalist platform and will arbitrarily reflect any ambient radio signal. However, the universal backscatter reader must do the “heavy lifting” in terms of signal acquisition, interference cancellation, decoding, and combining the multiple backscatter carriers to recover the sensor data, for eventual transport over the internet.

In this work the Universal Backscatter Reader consists of two, dual channel Ettus X310 Software Defined Radios equipped with UBX-160 daughterboards allowing for reception of frequencies from 10 MHz to 6 GHz. Given the host computers data throughput constraints, the maximum achievable sampling rate for each of the four receivers is 66.66 MHz, resulting in a UBRs total instantaneous bandwidth of 266 MHz. One of the four SDR receivers is assigned to cover the entire FM radio band from 80 to 110 MHz, and a second receiver covers a majority of the cellular uplink and downlink bands with operation from 814MHz to 881MHz. As will be discussed in more detail the remaining two receivers cover the ASTC digital TV bands from 514MHz to 580MHz in order to perform active carrier cancellation. Details on the signal-processing pipeline are presented in the following sections, and real world results are presented in section VI.

IV. UWB BACKSCATTER SIGNAL PROCESSING APPROACH

In traditional backscatter systems such as UHF RFID the reader generates the waveform that carries the backscatter signal. Thus, important factors such as carrier amplitude, data modulation, and phase constants are known, greatly simplifying the recovery of the backscatter data. However, in the case of ambient backscatter systems the carrier signal parameters generated by the broadcast system are unknown to the Universal Backscatter Reader and often suffer from a significant amount of multi-path interference since they may have been generated from a tower several kilometers away.

Figure 4 shows a block diagram of the receiver signal chain. The following subsections describe the *signal processing* sub-blocks used to decode the backscatter data that appears on top of the various broadcast system carriers. The maximum ratio combining with interference compensation block will be presented later in section V.

A. Analog FM Radio

FM broadcast radio stations transmit constant envelope radio signals that use frequency modulation to encode data. In the US the FCC has designated 100 channels from 87.5 to 108 MHz each with 200 KHz of bandwidth. The transmitter frequency modulation can be described as:

$$x(t) = A \cos(2\pi f_c t + 2\pi K_f \int_0^t m(\tau) d\tau) \quad (1)$$

Where $m(\tau)$ is the broadcast message and K_f represents the frequency sensitivity. A message $m(\tau)$ is sent by transmitting a varying frequency with a scaling factor K_f , while the envelope of the signal remains a constant value A . Figure 5, panel ‘A’ shows a typical FM radio signal captured with a Software

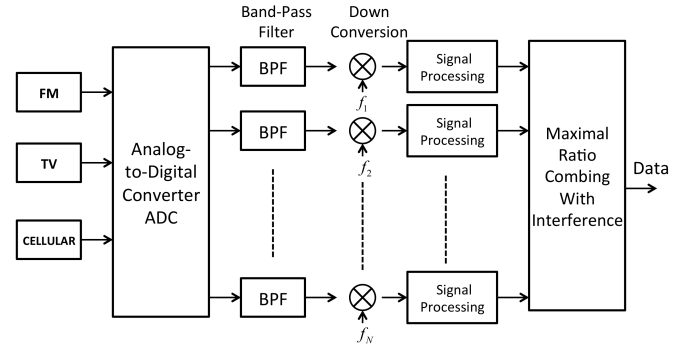


Fig. 4. The receiver signal processing pipeline receives digitized samples of wideband RF waveforms from FM, TV, and Cellular broadcasts. Each waveform is separated using an appropriate band pass filter, several operations are performed to extract the backscatter signal, and finally the individual signals are summed together using a Maximum Ratio Combining technique with interference cancellation.

Defined Radio. It should be noted that a significant amount of high frequency multi-path interference, as well as slow channel fading, is present on the signal making it difficult to decode the amplitude modulated backscatter data riding on top of the FM wave form. Thus in order to decode the embedded data in an FM signal a four step process is done consisting of: 1) envelope detection, 2) low pass filtering to remove the high frequency interference, 3) curve fitting technique tracking slow changes in the envelope 4) thresholding and data recovery.

1) *Envelope Detection*: decode an embedded backscatter signal, first we apply an envelope detection algorithm to the decoded backscatter signal at baseband [9], [12], [17]. An ambient radio signal with embedded backscatter modulation, that is down converted and sampled at the I and Q channels can be written as:

$$\begin{aligned} y_I[n] &= A \cos(\theta[n] + \phi) + B[n] \cos(\theta[n] + \gamma_z + \varphi) \\ y_Q[n] &= A \sin(\theta[n] + \phi) + B[n] \sin(\theta[n] + \gamma_z + \varphi) \end{aligned} \quad (2)$$

Where ϕ is a random phase offset due to the relative phase difference between the local oscillator (LO) and the incoming signal $x(t)$ while $\theta[n]$ is FM modulation message from $2\pi K_f \int_0^t m(\tau) d\tau$ after the sampling process. In addition, $B[n]$ is the backscatter signal waveform, γ_z is the constant phase offset from backscatter reflection and φ is the phase difference between the LO and backscatter signal. It should be noted that ϕ and φ are dependent on the distance between the reader and backscatter device. Next, the envelope of the FM signal is computed by taking the magnitude of the I and Q channels.

$$\begin{aligned} &\sqrt{y_I[n]^2 + y_Q[n]^2} \\ &= \sqrt{A^2 + B[n]^2 + 2AB[n] \cos(\varphi - \phi + \gamma_z)} \\ &= \|\vec{A} + \vec{B}[n]\| \end{aligned} \quad (3)$$

This result shows that indeed the amplitude of the enveloped signal is only dependent on the amplitude of \vec{A} (which should be constant) and the amplitude of the backscatter signal $\vec{B}[n]$.

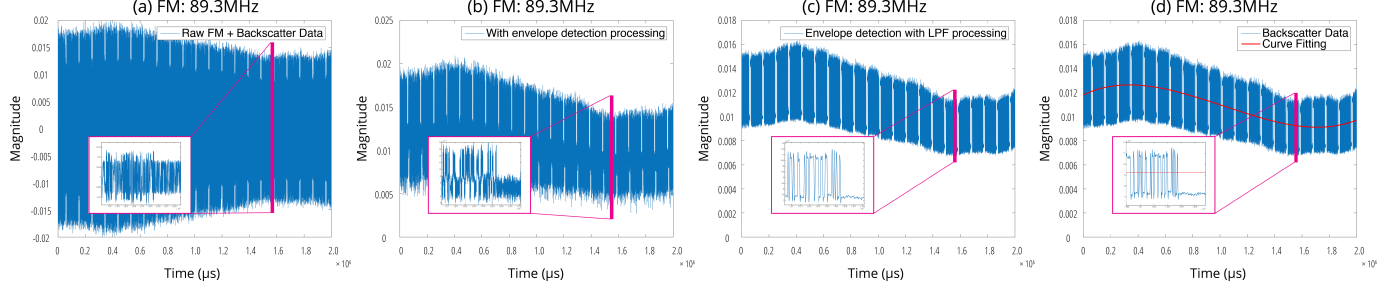


Fig. 5. Several signal processing stages are required to decode embedded backscatter data. Panel (a) shows a raw FM Signal with embedded backscatter data, panel (b) shows the same signal after envelope detection, panel (c) shows the output of the low pass filter, and panel (d) shows the result of curve fitting and the decoded data above and below the threshold.

However, as Figure 5 panel ‘B’ shows the real world FM radio waveform is not constant and thus further signal processing is necessary.

As a side note: for a backscatter signal $B[n]$ with digital amplitude modulation of $(0, V_B)$ the reader will experience dead zones as a function of reader-to-node distance, when $\cos(\varphi - \phi + \gamma_z) \approx \frac{-V_B}{2A}$. This is a known problem for all non-coherent (aka envelope detecting) backscatter readers [18], since the phase of the carrier is unknown. This can be a significant problem for narrow band ambient backscatter systems and will result in sinusoidally repeating nulls. However, this is not an issue for ultra wide-band ambient backscatter systems, since they use multiple ambient carriers at different frequencies and each ambient radio source has different distance to backscatter node as well as the reader resulting in different phase offset.

2) *Low-Pass Filter*: Due to the long distances associated with FM broadcast systems (10s of kilometers) there can be multiple transmission paths (due to reflectors in the environment) that will accumulate significant time delays. These multiple paths will be summed at the receiver resulting in a significant amount of high frequency noise, as can be seen in the zoomed ‘pop out’ window in 5 panel ‘B’. To mitigate this issue, a low-pass filter using the bandwidth of the backscatter signal is applied to the enveloped received signal such that the high frequency components (fast fading) can be removed as depicted in Figure 5 panel ‘C’.

3) *Curve-fitting*: The remaining low frequency components results in slow envelope changes (slow fading), which has sufficiently large amplitude over time to result in errors when thresholding the analog backscatter signal into 1s and 0s. To over come this issue a curve-fitting approach is used to create a dynamically changing threshold. The results can be seen in 5 panel ‘D’ which shows the red curve fit line which is able to accurately threshold the backscatter data.

B. ATSC TV System

The Advanced Television System Committee (ATSC) standard is a broadcast digital TV system used in North America which occupies a frequency band from 200 - 700 MHz. ATSC uses 8VSB, a vestigial sideband amplitude modulation scheme with 6 MHz of bandwidth and eight different signal levels

defined as $\pm 7, \pm 5, \pm 3$, and ± 1 . To synchronize the carrier frequency and normalize the amplitude, the ATSC system inserts a pilot which has a constant value of 1.25. The ATSC baseband signal $a(t)$ is a amplitude modulation waveform with a DC component. While \tilde{a} is the Hilbert transform of $a(t)$ with no DC component. An ATSC signal is defined as

$$\begin{aligned} \text{ATSC: } & a(t) \cos(2\pi f_{ct}) - \tilde{a}(t) \sin(2\pi f_{ct}) \\ & = \sqrt{a(t)^2 + \tilde{a}(t)^2} \cos(2\pi f_{ct} + \tan^{-1}(a(t)/\tilde{a}(t))) \end{aligned} \quad (4)$$

An ATSC signal has non-constant envelope; thus in addition to envelope detection, ATSC signals require a cancellation technique to remove the interference induced by amplitude modulation. However, ATSC contains a DC pilot which can be viewed as a single frequency tone with constant envelope. Thus, we develop two different decoder approaches that use either a single or multiple receivers.

1) *Single Receiver with Low Pass Filter*: By utilizing DC pilot information, we can estimate carrier frequency f_c [19]. Since an ATSC contains amplitude modulation in addition to the DC pilot, we can smooth the impact of AM by applying a low-pass filter as in the FM approach. This approach only requires a single antenna. Although we can estimate the frequency carrier via DC pilot, the AM modulation causes a the receiver to be unable to remove the radio source. Hence, the remaining components of the AM signal reduce backscatter performance.

2) *Dual Receiver Cancellation*: When two or more receivers are used, the AM modulation interference can be cancelled with dual receivers sampling from a common local oscillator. Signals acquired from coherent receivers are defined as y_{I_1}, y_{Q_1} and y_{I_2}, y_{Q_2} where y_{I_i}, y_{Q_i} is the I, Q channel at the i_{th} receiver, then the joint receiver decoding approach is

$$\text{LPF} \left[\sqrt{y_{I_2}[n]^2 + y_{Q_2}[n]^2} \times \frac{w_1}{w_2} - \sqrt{y_{I_1}[n]^2 + y_{Q_1}[n]^2} \right] \quad (5)$$

The coefficients w_1 and w_2 in (5) is the DC pilot amplitude value of the received signals I_1, Q_1 and I_2, Q_2 respectively. The DC pilot amplitude can be obtained by simply average a sequence of incoming ATSC data [19]. Once the DC pilot

amplitude is obtained, the amplitude of the received signal can be quantized to the same value for cancellation. For both the single and coherent receivers, we apply the curve fitting approach described earlier to mitigate slow fading.

C. Cellular Service

The radio system for mobile phones in North America is operated in three different frequency bands at 850, 1800, and 1900 MHz. The 850 MHz frequency band provides the longest range and best coverage capability, while 1800 and 1900 MHz has less interference for better signal quality. Generally, 850 MHz is the most popular frequency band for phone call services. In the cellular service, GSM, UMTS and CDMA2000 are the main systems for mobile phone. GSM uses frequency shift keying modulation (FSK) with time division multiple access (TDMA) to share the channel across multiple phones and results in non-continuous traffic. Unlike GSM, both UMTS and CDMA2000 utilize phase-shift keying (PSK) with code division multiple access (CDMA) to share the channel; these systems generate continuous traffic and have the constant envelope property. A common phase-shift keying modulation used for the CDMA technique is:

$$\text{PSK}: R(t) \cos(2\pi f_c t + \varphi_i) \quad (6)$$

where $R(t)$ is used for power control while the φ_i in (6) is the phase information to send a sequence of number known as CDMA chip sequence. The chip sequence rate in CDMA2000 is 1.2 Mcps while UMTS is 3.8 Mcps [20], [21].

To compensate the fading channel influence for both downlink and uplink, the cellular system applies a power control mechanism to maintain a minimum power level on the receiver side. Thus, the amplitude $R(t)$ in (6) is no longer constant amplitude. Instead, the amplitude $R(t)$ is a time-varying step function with typically 1dB to 3dB amplitude levels. The rate that inner loop power control is applied is 1500 Hz for UMTS and 800 Hz for CDMA2000; outer loop control is applied at a much slower rate of 10-100 Hz. Since a backscatter signal's data rate is much higher than 800 or 1500 Hz the received signal during each step of $R(t)$ time duration can be viewed as a constant. Therefore, by applying the previously described curve-fitting approaches, the non-constant envelope from power control can be mitigated.

V. MAXIMIZING SIGNAL PERFORMANCE WITH MULTI-CHANNEL COMBINATION

The previous section showed how to decode backscatter signals embedded in different radio systems in isolation. Since an ultra-wideband backscatter nodes can simultaneously embed its data on top of multiple frequency bands, across different radio broadcast systems, there is the opportunity to combine all these sources to improve signal strength and performance. However, as previously described each backscatter channel experiences different interference and signal strength. Combining these signals requires a framework that can assign a weight to each frequency channel that yields an optimal combination.

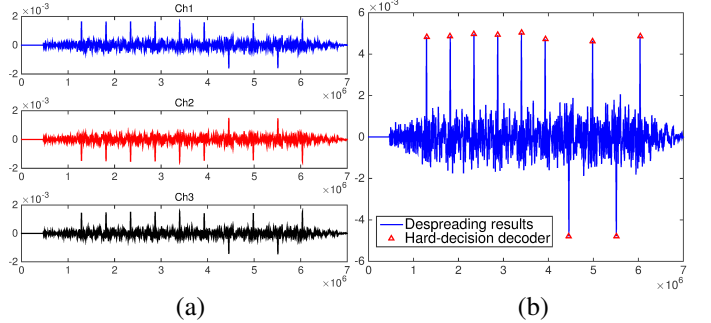


Fig. 6. In panel (a), we show signals on three different backscatter channels that contain the same data; channel 2 is inverted since its polar direction is reversed. Panel (b) shows these three signals summed together using MRC after polarity compensation.

A. PN Sequence Polar Correction

Figure 4 presents the overall structure of a wideband receiver where a bandpass filter selects the frequency band with a corresponding backscatter signal. To later combine received backscatter signals, the embedded data is spread using a Pseudo-Noise (PN) sequence. This approach increases signal robustness to interference and also assists in synchronization by enabling peak detection. A similar concept can be found in a Rake receiver [22], which utilizes despreading to estimate sub-receiver status for combination. The main difference between our receiver and a Rake receiver is that we do not apply time delay compensation, since our backscatter signals come from different frequency channels rather than different paths which have multipath delay spread.

When backscatter signals from different channels arrive at the same receiver, some channels may be inverted as a result of differing frequency components and phase offsets. To address this, we define a preamble with known polar direction to compensate. Figure 6 (a) shows a backscatter signal after processing and despreading a PN sequence transmitted on three different channels. Channels 1 and 3 have the same polar direction, while channel 2 is inverted. To correct the signal's polarity, the receiver needs ground truth; specifically, the backscatter node prepends a fixed length bit sequence as a preamble to each packet. When a backscatter node transmits, the receiver uses the preamble to correct the polarity, thus enabling the channels to be added together. In our implementation we chose a preamble of [1, 1, 1, 1, 1]. In the next section, we will show how to select optimal weights for channel combination.

B. MCR with Carrier Interference Compensation

To sum backscatter signals acquired from different channels, we apply a modified version of maximal ratio combining (MRC) that suppresses the interference caused by the ambient carrier. The general principle of MRC is that the signal gain of each channel is adjusted such that it is proportional to the signal to noise ratio of that channel. For example, a conventional Rake receiver utilizes a PN sequence to combine a narrow band signal from multiple paths; a weighted channel

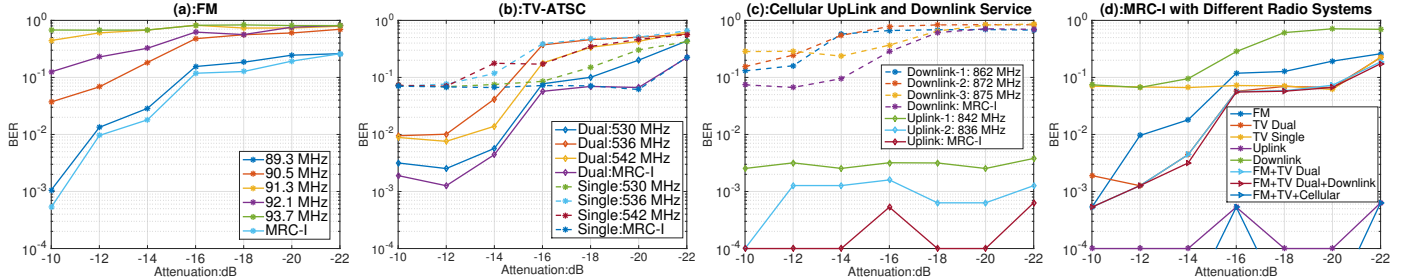


Fig. 7. The performance of our receive pipeline is evaluated by replaying ambient signals with different levels of attenuation. We measure BER for: (a) FM (b) ATSC Television (c) Cellular Downlink & Uplink, and (d) MRC-I

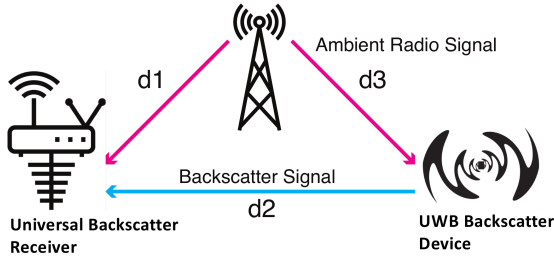


Fig. 8. Ambient backscatter systems utilize existing radio sources for communication. A backscatter device embeds data in a continuous waveform, which can be detected and decoded by a reader.

is assigned to each receiver finger to combine the signals [23]. Thus, by leveraging the same concept, we can view each independent frequency channel as a finger in our Universal Backscatter Receiver.

However, in our application, each channel not only has its own embedded backscatter signal strength, but also has different levels of interference across each ambient radio source; therefore, MRC should consider both of these factors. Prior art [11] uses MRC for multiple channel combination by only considering noise as a disturbance; instead we view the MRC problem as co-channel interference which is illustrated in greater detail in [24]. Thus, to achieve the optimal combination of L channels in a interference environment, we have maximal ratio combining under the interference of ambient radio sources as (MRC-I):

$$\text{MRC-I: } \sum_{i=1}^L ch_i * \frac{V_i}{\sigma_I^2 + \sigma_N^2} \quad (7)$$

where V_i is the average peak amplitude of the signal after the despreading process, indicating the signal strength of each channel. In Equation 7, parameters σ_I^2 and σ_N^2 refer to the interference from ambient radio noise components respectively while ch_i is the despreading result for each channel i as shown in Figure 6 (a). To estimate these parameters, we calculate the variance of the received ambient radio sources with no embedded backscatter data. Since we can use the peak position from the output of the despreading operation to identify a backscatter packet, we also select a time interval without containing backscatter signals (i.e. the time interval between consecutive backscatter packets) to perform the estimation.

To precisely estimate the interference from ambient radio sources and noise components, we compute the variance of the ambient radio signal prior to applying the despreading operation. This approach is used since each sample, after the despreading process, has less signal contribution from the ambient radio source and most samples may contain peaks from partial backscatter signals. The computed variance refers to a combination of noise and interference, since the interference and noise components are independent from one another.

After summing all radio sources with corresponding weight factors, the result is shown in Figure 6(b). After combining, the receiver can use a hard-decision to obtain a binary data stream. In some cases, the preamble or signal peak cannot be found since the interference is much larger than the signal; in this case, a weight of 0 can be assigned. By doing this, we can remove frequency channels that contain only noise to improve performance. One should also note that if there is no co-channel interference components from ambient radio sources (i.e no multipath), the weight factor in equation 7 becomes $\frac{V_i}{\sigma_N^2}$, which is the original MRC formulation.

C. MRC Performance Benchmarks

In order to evaluate the performance of the MRC-I technique in a controllable and repeatable manner, we perform a series of bench top tests. First, we recorded FM, ASTC, and mobile downlink and uplink radio sources in our office and later replay each radio source normalized to the same signal strength. To model changes in ambient radio strength and interference, we use two transmitters replaying the same radio waveform content to act as the radio sources in paths d_1 and d_3 individually in Figure 8. Then, we assigned the same gain of ambient radio source in both path. The distance in path d_2 is modeled by using an attenuator; by using the Friis equation, we can simulate longer distances by applying more attenuation. For repeatability in our experiments paths d_1 , d_2 and d_3 all use RF coax cable instead of free space propagation. For each trial, we collect ~ 2 kbytes of backscatter data to calculate the average bit error rate (BER).¹

¹In our evaluation, we simply calculate BER as the number of bits that are unable to be detected over the total number of received data samples. If no packet with a valid preamble is detected over all of the received samples, the BER is 1. If all data bits are successfully detected, we set the BER to 10^{-4} instead of 0, because our sample scale only reaches 10^{-3} .

Figure 7 (a-c), shows the bit error rate as a function of varying attenuation levels for backscattered data transmitted on top of multiple channels of a particular radio broadcast system and the performance improvement achieved using MRC-I. Figure 7(d) shows the BER achieved using MRC-I for each radio system in isolation, as well as combining all the broadcast systems together using MRC-I. The BER performance of a decoding strategy that uses only FM in panel (a) shows that despite normalization, each channel path performs proportional to the amount of multipath interference. In contrast, MRC-I achieves lower BER than the worst channel across all attenuation levels; this demonstrates that MRC-I is boosting the SNR through channel combining. In panel (b), we observe similar performance results for the ATSC radio system; we note that as expected, the dual receiver outperforms the single receiver for each channel in isolation, as well when using the MRC-I technique. In panel (c), we show that performance results from cellular show a similar trend as the previous systems, but we note that there is a substantial difference between uplink and downlink performance. Since the mobile phone is nearby, the uplink suffers from significantly less multipath interference. Finally, panel (d) shows the performance achieved by MRC-I when combining various radio systems. When MRC-I is able to use all available radio sources simultaneously, it achieves a lower BER than any of the systems in isolation – this is a strong indication that our ultra-wideband approach can greatly improve ambient backscatter performance.

VI. SYSTEM IMPLEMENTATION AND INDOOR PERFORMANCE EVALUATION

In this section, our goal is to prove the real world performance of our ultra-wideband ambient backscatter approach using MRC-I. Towards this aim, we perform experiments in 14 different locations in an indoor office environment, depicted in Figure 9. Across all experiments, we use ambient signals generated by the 14 radio towers shown in Figure 2; additionally, we use 2 mobile phones to measure the performance contributions of cellular uplink channels – for this purpose we use an HTC Droid Incredible (Verizon) and a Google Nexus 5 (AT&T) to generate CDMA2000 and UMTS uplink signals respectively. We place the HTC phone 1 meter away from location C and 3 meters away from location D in Figure 9; we placed the Nexus 5 40 cm away from location Z.

In our experimental setup, the backscatter device (depicted in Figure 3) uses PN sequence chip rates of 10 and 66 KHz. The PN sequence used is a Gold code sequence, which is widely used in CDMA technology due to its low auto correlation property. Additionally, we use two different PN sequence lengths of 63 and 127 chips. Combining these chip lengths and rates, we have four unique data rates, denoted as D1: 1.04 Kbps (66K/63), D2: 0.52 Kbps (66K/127), D3: 158.7 bps(10K/63), and D4: 78.4bps (10K/127) to measure performance. We move the transmitting backscatter node to each of the locations shown in Figure 9. To receive data from the

node we deploy the Universal Backscatter receiver at a fixed location as indicated on the map.

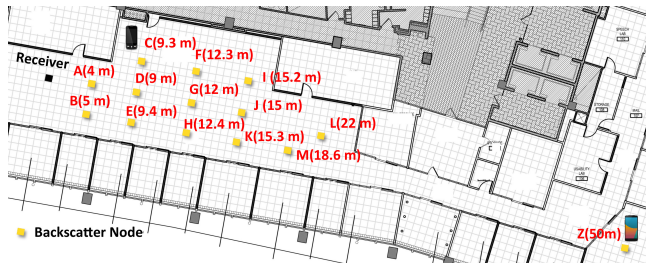


Fig. 9. In our experiments, the UBR was placed in a fixed location denoted by the black square; the backscatter node was moved to 14 different locations denoted by the yellow markers. A mobile phone was placed at locations C and Z to measure the contribution of cellular uplink channels.

FM-1	FM-2	FM-3	FM-4	FM-5	FM-6
-44 ± 3	-42 ± 3	-65 ± 7	-85 ± 10	-65 ± 5	-80 ± 7
TV-1	TV-2	TV-3	TV-4	TV-5	TV-6
-75 ± 10	-86 ± 12	-92 ± 10	-68 ± 10	-72 ± 10	-74 ± 10
Cell-1	Cell-2	Cell-3	Phone ≤ 0.5 m	$1 \text{ m} \leq \text{Phone} \leq 3$ m	$\text{Phone} \geq 3$ m
-90 ± 5	-95 ± 10	-85 ± 5	-30 ± 3	-50 ± 5	-65 ± 10

TABLE I
Measured signal strength values from different radio systems and channels across all indoor locations (units: dBm)

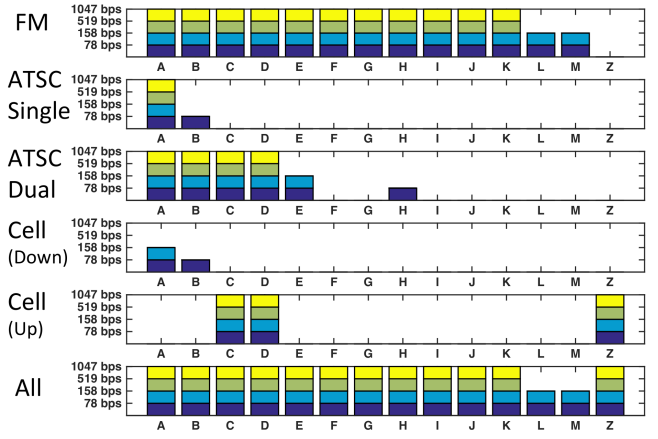


Fig. 10. We report the data rates achievable by different receiver strategies across all indoor locations. We indicate a successful read range when the measured BER is $<10^{-2}$.

For FM radio signals, the receiver is able to observe the entire FM frequency band from 80 to 110 MHz. For ATSC signals, the observable frequency is from 517 to 583 MHz. For mobile services, the measured frequency range is from 814 to 880 MHz which covers most uplink channels and some of the downlink services. We measured our system performance at 14 different indoor locations listed in Figure 9. Table I lists the signal strength profile for each ambient radio source as measured by using a Rohde & Schwarz SMIQ03B frequency spectrum analyzer in our indoor environment.

Figure 10 presents the overall performance using MRC techniques with respect to different radio systems by using $\text{BER} < 10^{-2}$ as the threshold for a valid read range. By utilizing 6 FM channels with MRC-I technique, a receiver can achieve a communication range of at most 22 meters (location L) at data rates of 78 and 158 bps, while at 15.3 meters, we achieve

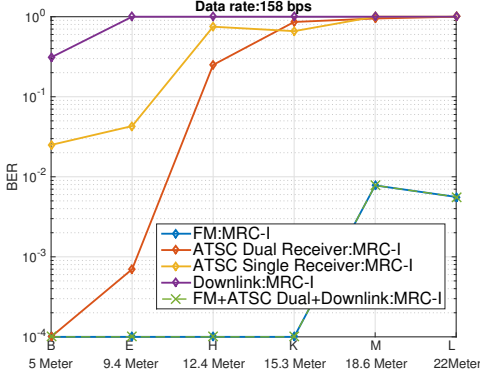


Fig. 11. We demonstrate the read range performance of different MRC strategies by plotting BER for a subset of measured distances. After combining FM, ATSC, and cellular downlinks, we achieve a BER of $<1\%$ at 22 meters.

data rates of 0.5 and 1.0 kbps. When the receiver utilizes the 6 ATSC channels, the maximum read range achieved is 12.4 meters (location H) and at the fastest data rate of 1 kbps achieve 9 meters of range. When utilizing a cellular uplink, we can achieve a read range of 50 meters at 1 kbps when the backscatter node is placed next to the phone; however we note that performance quickly degrades as the transmitter moves away from the phone (see Figure 10). When combining all radio systems (FM, ATSC, cellular uplink, and cellular downlink), we can decode data transmitted by a node placed at any of the indoor locations. Finally, in Figure 11 we illustrate the BER with respect to distance by displaying a subset of locations when using the 159 bps data rate. At longer distances, all radio systems suffer from performance degradation. By using the MRC-I technique with all radio sources and channels, we can provide more locations with backscatter communication service.

VII. CONCLUSION

Ultra wideband ambient backscatter retains the power reduction benefits of narrow band backscatter systems while offering a number of key benefits. For instance by spreading the backscatter signal power across multiple spectral components (i.e. ambient sources) it is possible to use our MRC-I algorithm with carrier interference cancellation to boost the signal to noise ratio. Results show that our system can achieve a read range of 22 meters at 158 bps, using 15 broadcast sources at power levels ranging from -90 to -39 dBm. When adding in ambient cellular uplink transmitter it is possible to achieve 50 meters of read range at 1047 bps. Additionally, since our system uses multiple carrier frequencies we can mitigate read nulls which effect narrow band non-coherent backscatter receivers resulting in a more robust system. Finally, UWB ambient backscatter offers the potential to be deployed in nearly any metropolitan area since the hardware does not have to be tuned for a particular frequency band.

REFERENCES

- [1] M. T. Lazarescu, "Design of a wsn platform for long-term environmental monitoring for iot applications," *IEEE Journal on Emerging and Selected Topics in Circuits and Systems*, vol. 3, pp. 45–54, March 2013.
- [2] S. Patel, H. Park, P. Bonato, L. Chan, and M. Rodgers, "A review of wearable sensors and systems with application in rehabilitation," *Journal of NeuroEngineering and Rehabilitation*, vol. 9, pp. 1–17, 2012.
- [3] S. Sudevalayam and P. Kulkarni, "Energy harvesting sensor nodes: Survey and implications," *IEEE Communications Surveys Tutorials*, vol. 13, pp. 443–461, Third 2011.
- [4] R. Vullers, R. van Schaijk, I. Doms, C. V. Hoof, and R. Mertens, "Micropower energy harvesting," *Solid-State Electronics*, vol. 53, no. 7, pp. 684 – 693, 2009.
- [5] Buettnner, *Backscatter Protocols and Energy-Efficient Computing for RF-Powered Devices*. PhD thesis, University of Washington, jun 2012.
- [6] A. P. Sample, D. J. Yeager, P. S. Powledge, A. V. Mamishev, and J. R. Smith, "Design of an rfid-based battery-free programmable sensing platform," *IEEE Transactions on Instrumentation and Measurement*, vol. 57, pp. 2608–2615, Nov 2008.
- [7] S. Naderiparizi, Y. Zhao, J. Youngquist, A. P. Sample, and J. R. Smith, "Self-localizing battery-free cameras," in *Proceedings of the 2015 ACM International Joint Conference on Pervasive and Ubiquitous Computing, UbiComp '15*, (New York, NY, USA), pp. 445–449, ACM, 2015.
- [8] E. Welbourne, L. Battle, G. Cole, K. Gould, K. Rector, S. Raymer, M. Balazinska, and G. Borriello, "Building the internet of things using rfid: The rfid ecosystem experience," *IEEE Internet Computing*, vol. 13, pp. 48–55, May 2009.
- [9] V. Liu, A. Parks, V. Talla, S. Gollakota, D. Wetherall, and J. R. Smith, "Ambient backscatter: wireless communication out of thin air," *SIGCOMM Comput. Commun. Rev.*, vol. 43, no. 4, pp. 39–50, 2013.
- [10] A. N. Parks, A. Liu, S. Gollakota, and J. R. Smith, "Turbocharging ambient backscatter communication," in *SIGCOMM Comput. Commun. Rev.*, vol. 44, pp. 619–630, ACM, 2014.
- [11] B. Kellogg, A. Parks, S. Gollakota, J. R. Smith, and D. Wetherall, "Wi-fi backscatter: internet connectivity for rf-powered devices," *SIGCOMM Comput. Commun. Rev.*, vol. 44, no. 4, pp. 607–618, 2015.
- [12] D. Bharadia, K. R. Joshi, M. Kotaru, and S. Katti, "Backfi: High throughput wifi backscatter," *SIGCOMM Comput. Commun. Rev.*, vol. 45, pp. 283–296, 2015.
- [13] B. Kellogg, V. Talla, S. Gollakota, and J. R. Smith, "Passive wi-fi: bringing low power to wi-fi transmissions," in *13th USENIX Symposium on Networked Systems Design and Implementation*, pp. 151–164, 2016.
- [14] J. F. Ensworth and M. S. Reynolds, "Every smart phone is a backscatter reader: Modulated backscatter compatibility with bluetooth 4.0 low energy (ble) devices," in *2015 IEEE Int. Conf. RFID*, pp. 78–85, 2015.
- [15] A. T. S. Committee, "Atsc recommended practice: Receiver performance guidelines," Tech. Rep. Document A/74:2010, Advanced Television Systems Committee, Inc., apr 2010.
- [16] P. V. Nikitin and K. S. Rao, "Theory and measurement of backscattering from rfid tags," *IEEE Antennas and Propagation Magazine*, vol. 48, no. 6, pp. 212–218, 2006.
- [17] P. V. Nikitin, S. Ramamurthy, R. Martinez, and K. Rao, "Passive tag-to-tag communication," in *2012 IEEE Int. Conf. RFID*, pp. 177–184, 2012.
- [18] P. V. Nikitin, S. Ramamurthy, and R. Martinez, "Simple low cost uhf rfid reader," in *Proc. IEEE Int. Conf. RFID*, pp. 126–127, 2013.
- [19] C. Y. Wu, *A software 8-VSB receiver for ATSC digital television*. PhD thesis, Massachusetts Institute of Technology, 1999.
- [20] H. Holma, A. Toskala, et al., *Wcdma for umts*, vol. 2. Wiley Online Library, 2000.
- [21] V. K. Garg, *IS-95 CDMA and CDMA2000: Cellular/PCS systems implementation*. Pearson Education, 1999.
- [22] S. Hara and R. Prasad, "Overview of multicarrier cdma," *IEEE communications Magazine*, vol. 35, no. 12, pp. 126–133, 1997.
- [23] M.-S. Alouini, S. W. Kim, and A. Goldsmith, "Rake reception with maximal-ratio and equal-gain combining for ds-cdma systems in nakagami fading," in *Universal Personal Communications Record*, 1997., vol. 2, pp. 708–712, IEEE, 1997.
- [24] J. Winters, "Optimum combining in digital mobile radio with cochannel interference," *IEEE Journal on Selected Areas in Communications*, vol. 2, pp. 528–539, July 1984.